Nanodosimetry of Auger electrons: A case study from the decay of ^{125}I and 0–18-eV electron stopping cross sections of cytosine

M. Michaud, M. Bazin, and L. Sanche
Département de Médecine Nucléaire et Radiobiologie, Faculté de Médecine et Sciences de la Santé, Université de Sherbrooke, Sherbrooke, Québec, Canada J1H 5N4
(Received 28 November 2012; published 4 March 2013)

Radiopharmaceuticals emitting Auger electrons are often injected into patients undergoing cancer treatment with targeted radionuclide therapy (TRT). In this type of radiotherapy, the radiation source is radial and most of the emitted primary particles are low-energy electrons (LEEs) having kinetic energies distributed mostly from zero to a few hundred electron volts with very short ranges in biological media. These LEEs generate a high density of energy deposits and clustered damage, thus offering a relative biological effectiveness comparable to that of alpha particles. In this paper, we present a simple model and corresponding measurements to assess the energy deposited near the site of the radiopharmaceuticals in TRT. As an example, a calculation is performed for the decay of a single ^{125}I radionuclide surrounded by a 1-nm-radius spherical shell of cytosine molecules using the energy spectrum of LEEs emitted by ^{125}I along with their stopping cross sections between 0 and 18 eV. The dose absorbed by the cytosine shell, which occupies a volume of 4 nm^3, is extremely high. It amounts to 79 kGy per decay of which 3%, 39%, and 58% is attributed to vibrational excitations, electronic excitations, and ionization processes, respectively.

DOI: 10.1103/PhysRevE.87.032701 PACS number(s): 87.53.Bn, 87.55.ne, 34.50.Bw, 87.55.de

I. INTRODUCTION

In cancer therapy, the ultimate goal is to deliver a sterilizing dose to all cancer cells in the body, while sparing nearby healthy cells [1]. For micrometastatic and disseminated diseases, which exhibit circulating single cells or clusters of cells, the method of choice is targeted radionuclide therapy (TRT) [2]. TRT requires suitable pharmaceutical carriers or targeting agents, such as peptides and monoclonal antibodies, aimed at tumor cells and labeled with the appropriate radionuclides (i.e., radiopharmaceuticals) [2,3]. Radionuclides that emit low-energy β particles, α particles, or Auger electrons seem to be more adequate as these particles, which are currently the primary particles in TRT, are generally characterized by a short range and a high linear energy transfer (LET) in tissue [4,5]. More particularly, radionuclides emitting low-energy Auger electrons having energies lower than a few hundred electron volts, and thus very short ranges in biological media, are also beneficial for minimizing radiotoxicity and damage to normal tissues. Such radionuclides appear to be most effective to treat selectively small tumors or disseminated metastases, when bound or incorporated into the DNA of cancer cells [6]. The reason is that the many emitted low-energy electrons (LEEs), generate a high density of energy deposits that induce double strand breaks and clustered damage in the immediate vicinity of the radionuclides [2], thus offering a relative biological effectiveness (RBE) comparable to that of high-LET α particles [4,5]. It appears that optimal TRT is not only limited to the design of suitable carriers, but also requires quantifying the energy imparted per unit mass (i.e., the absorbed dose) by such radionuclides at the single-cell level with an emphasis on the DNA structure. Historically TRT has been based mainly on semi-empirical formulas and techniques to determine radiation doses [7]. Only recently were dose calculations based on elementary processes presented and entered practical applications [8,9]. Therefore, correct experimental and theoretical cross section (SC) data for [10–15] LEEs' interaction with biomolecules are essential for such calculations, so as to provide not only the deposited energy and damage distributions within a cell, but also to link more directly these distributions to the RBE [16].

In the present work, we present a simple model based on the medical internal radiation dose (MIRD) schema [17] to perform the nanodosimetry of the decay of a single ^{125}I radionuclide surrounded by a 1-nm-radius spherical shell of cytosine molecules using the energy spectrum of LEEs emitted by ^{125}I along with their stopping cross section (SCS) values between 0 and 18 eV. Since different DNA subunits have similar electron energy-loss CSs [18–27], the calculation should provide an estimate of the dose absorbed by DNA molecules under similar conditions.

II. METHODS

A. MIRD schema

The absorbed dose is the central quantity for assessing and predicting the efficacy of any radiotherapeutic modality. According to the MIRD schema [17], the mean dose absorbed by a target region k from activity in a source region h can be written as [28–30]

$$D_{k\leftarrow h} = \tilde{A}_h S_{k\leftarrow h}, \tag{1}$$

where $\tilde{A}_h$ is the cumulated activity, representing the sum of all nuclear decays taking place in the source region h. As such, it depends on the half-life of the radionuclide and various physiological and biological factors related to the kinetics of its carrier within the body. The quantity $S_{k\leftarrow h}$ is an absorbed dose of the target region k produced by a unit nuclear decay in the source region h. It is given by

$$S_{k\leftarrow h} = \frac{\Delta\varphi_{k\leftarrow h}}{M_k}, \tag{2}$$

where the quantity Δ is the energy emitted by the radionuclide per disintegration, $\varphi_{k\leftarrow h}$ the fraction of energy emitted by the radionuclide in the source region h and absorbed in the target region k, and M_k the mass of the target volume k. The product of Δ and $\varphi_{k\leftarrow h}$ depends on the spectrum of the particles emitted by the radionuclide and their interaction CSs with the target k. Hence it is a purely physical quantity whose calculation may proceed irrespective of any knowledge on $\tilde{A}_k$.

The utility of the MIRD schema lies in its simplicity and general applicability. No assumptions are made regarding the composition, geometry, or dimensions of the source or target [29,31]. Although used normally for macroscopic volumes, such as organs, this formalism may also be applied to smaller objects, such as subcellular components, at the nanoscopic scale [32]. In the case of TRT using Auger emitters that produce LEEs having energies less than a few hundred electron volts with a mean free path (MFP) smaller than a micrometer, the volume of energy deposited around the radionuclide has microscopic or even nanoscopic dimensions. Also, the distribution of the radiopharmaceuticals absorbed in the cancer cells being very heterogeneous, the total dose is the sum of the nanoscopic doses absorbed around all heterogeneities. Therefore, to carry out dosimetry or more specifically nanodosimetry in the presence of these radiopharmaceuticals requires the knowledge of the electron energy-loss (EEL) spectra of the constituents of DNA and the corresponding CS values for LEEs to deposit their energy.

The radionuclide ^{125}I releases per decay on average 25 Auger electrons whose frequency distribution $N(E_0)$ as a function of the energy of the Auger electron E_0 below 18 eV (i.e., the energy spectrum of Auger electrons) is reported in Table I [33,34]. The idealized model of DNA, shown in Fig. 1, is defined as 1-nm radius R spherical shell of cytosine of surface number density n_s with the ^{125}I decaying at its center. Given this simple geometry, it can be shown that Eq. (2) for the absorbed dose per a unit nuclear decay (i.e., $\tilde{A}_h = 1$) takes the following form

$$S_{k\leftarrow h} = \underbrace{\frac{1}{4\pi R^2 n_S m_{Cy}}}_{M_k} \sum_{E_0} \overbrace{N(E_0)E_0}^{\Delta} \overbrace{\sum_i \sigma_i(E_0)\frac{\varepsilon_i}{E_0} n_S}^{\varphi_{k\leftarrow h}}, \qquad (3)$$

where ε_i is the energy of the excitation mode i of the molecule (i.e., EEL features), $\sigma_i(E_0)$ is the integral CS to deposit the energy ε_i into the excitation modes i, and m_{Cy} is the molecular mass of cytosine (i.e., 111.1 amu). Recognizing that both factors E_0 and n_s appear in the numerator and denominator on the right-hand side of Eq. (3), the latter equation simplifies to

$$S_{k\leftarrow h} = \frac{1}{4\pi R^2 m_{Cy}} \sum_{E_0,i} N(E_0)\sigma_i(E_0)\varepsilon_i. \qquad (4)$$

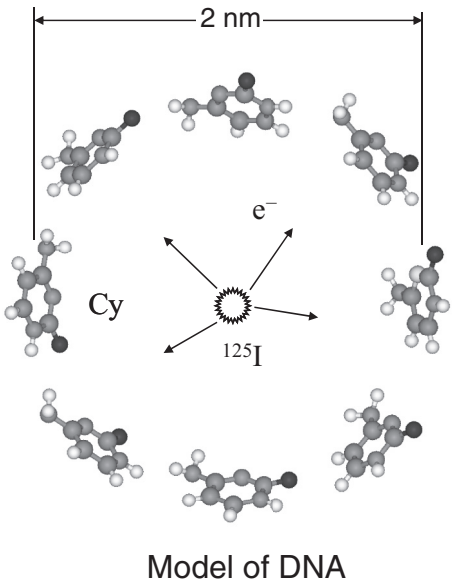

FIG. 1. Idealized model of DNA defined as 1-nm-radius spherical shell of cytosine with a ^{125}I decaying at its center.

In this expression, the product of $\sigma_i(E_0)$ and ε_i associated with the electron-molecule scattering process i is defined as the SCS [35]. The sum over i may be thought of as the mean energy loss per unit pathlength of a particle penetrating a medium of unit molecular number density. This is the quantity necessary to assess the energy deposition process of a moving particle losing its energy and momentum through a series of inelastic scatterings with the constituent molecules of the medium and eventually being stopped. Finally, it can be seen that the ratio of $\sigma_i(E_0)$ to $4\pi R^2$, where R is the distance between the radial source h and the target k, corresponds to an effective solid angle of the cytosine molecule.

B. Cross section data

Several experimental studies were undertaken recently by our group to determine the *absolute* CSs for vibrational and electronic excitations of individual DNA subunits (e.g., a base or a sugar) by LEE impact [18–27]. In our experiments an electron beam of current I_0 and energy E_0 provided by a monochromator is incident on a thin film made of molecules of a specific basic DNA subunit. The film is prepared under UHV conditions by sublimation onto an inert solid Ar substrate using a double-stage oven system [21]. The current of electrons backscattered in the direction θ_d is measured by an analyzer as a function of the energy transferred E - E_0 to the molecules. Under single collision and normal incidence conditions, it can be shown that the expression for such a current energy

TABLE I. Frequency distribution $N(E_0)$ as a function of the Auger electron energy E_0 (eV) below 18 eV for the nuclear decay of a single ^{125}I.

	$N(E_0)$[a]																	
	2	0.3	0.08	0.5	0	0.15	0.1	0.2	0.1	0.07	0.08	0.1	0.15	0	0.07	0.1	0.04	0.04
E_0	1	2	3	4	5	6	7	8	9	10	11	12	13	14	15	16	17	18

[a]From Fig. 1 of Ref. [34].

distribution also called EEL spectrum reduces to

$$I(\theta_d, E_0, E - E_0) \cong I_0(\theta_d, E_0)\sigma_r(E_0, E - E_0)n_S. \quad (5)$$

Here $I_0(\theta_d, E_0)$ is an effective incident electron current, which may be seen as the portion of the incident electron current I_0 that would be backscattered into the analyzer in the same direction θ_d by a material having an elastic reflectivity equal to 1. In practice, it is obtained from extrapolating the linear relationship found between the total reflected (i.e., energy integrated EEL spectrum) and transmitted currents as a function of increasing molecular coverage on the substrate. The quantity $\sigma_r(E_0, E - E_0)$ is a CS per unit energy transfer for an electron of energy E_0 to deposit an energy E - E_0 into a molecule and be backscattered over the whole half-angular space (i.e., the differential CS integrated over the whole half-angular space in the backward direction). Finally n_S is the surface number density of molecules on the substrate. Given $I_0(\theta_d, E_0)$ and n_S, the quantity $\sigma_r(E_0, E - E_0)$ obtained from the above expression for the EEL spectrum is then fitted with multiple Gaussian functions to delimit the various excitation energy regions. Finally, the CSs to deposit energy into the various excitation modes i of the molecule by electron impact $\sigma_{ri}(E_0)$ are obtained from the areas under the corresponding Gaussians' distributions. For an electron having the same probability to be scattered in the backward and forward direction, with respect to the molecular film surface (i.e., isotropic scattering), $\sigma_{ri}(E_0)$ accounts for half of the integral CS $\sigma_i(E_0)$.

III. RESULTS AND DISCUSSION

The SCS values can readily be computed from the experimental data for LEE scattering from cytosine [25–27]. In Fig. 2, we report the electron impact energy dependence of the SCSs for the vibrational excitation, electronic excitation, and ionization between 0 and 18 eV. The large differences in magnitude for the SCSs of the various excitation processes show that different underlying physics governs the energy-loss process above and below the electronic excitation threshold. Above the electronic excitation threshold, a LEE loses a relatively large amount of kinetic energy per collision through

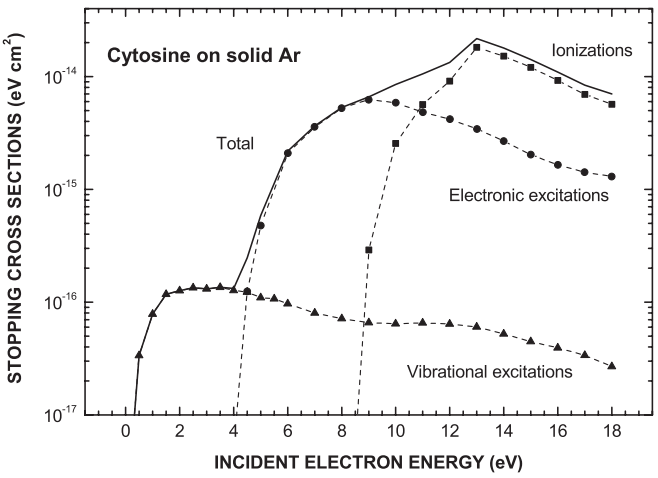

FIG. 2. Low-energy electron stopping cross sections for the vibrational excitations, electronic excitations, and ionizations of cytosine.

TABLE II. Dose absorbed (kGy) by a spherical shell of cytosine along with the contribution to the different excitation processes, upon the decay a single ^{125}I. The values in parentheses are the relative contribution in percentage (%).

	Excitation mode			
	Vibration	Electronic	Ionization	Sum
Absorbed Dose	2.5 (3)	31 (39)	45.5 (58)	79 (100)

electronic excitations and ionizations of the medium. Ions and electronically excited species formed by LEEs are often chemically active and cause significant changes in neighboring molecules. On the other hand, LEEs with a kinetic energy below electronic excitation thresholds lose smaller amounts of kinetic energy per collision through the excitation of vibrational and phonon modes. They are primarily responsible for producing vibrationally excited species as well as forming anions and radicals via dissociative electron attachment [36]. While the latter products are known for their high reactivity [37], some vibrationally excited molecular species, even those with a single quantum of excitation, react much faster than species in the vibrational ground state. Thermally excited species usually interact relatively slowly with the surrounding atoms and molecules through thermal chemical reactions, often causing milder consequences to the medium.

Taking the SCS values (Fig. 2) and the frequency distribution of LEEs in Table I, the initial dose (i.e., $< 10^{-14}$ s) absorbed by the spherical shell of cytosine is calculated from Eq. (4) and reported in Table II, along with the contributions to the different excitation processes. The major contribution is found to arise from electronic excitation and ionization. Although the frequency distribution below the electronic excitation energy threshold accounts for 75% of the electrons (Table I), the vibrational contribution amounts only to 3% of the dose. This result arises essentially from the fact that the SCS values for the vibrational processes are up to two orders of magnitude smaller than those for the electronic excitation and ionization. Still, this outcome would not have been much different, if the secondary electrons produced by the ionization processes had been added to the number of LEEs below the electronic excitation threshold.

IV. CONCLUSION

The assessment of biological risks associated with internal administration of radiopharmaceuticals assumes a homogeneous uptake in source organs and a uniform absorbed dose distribution in target organs [38]. This conventional dosimetry, which is valid only for macroscopic volumes at the level of tissues and organs (cm - mm), is thus unable to provide the needed micro- or nanodosimetry for TRT. In fact, biological studies have shown differences in the uptake and clearance of the radiopharmaceuticals among cells in a given tissue [39]. Furthermore, radionuclides have been found to be selectively localized in particular subcellular critical structures (e.g., cell nucleus, the chromosome, or bound to DNA), depending on the biological properties of the targeting agent [2,40]. This heterogeneous uptake has no dosimetric consequences in the case of long-range radiation such as photons [41]. However,

most radionuclides used in nuclear medicine for medical imaging and cancer therapy (e.g., ^{67}Ga, ^{99m}Tc, ^{111}In, ^{123}I, ^{125}I, and ^{201}Tl) emit not only photons but also low-energy Auger electrons [42,43]. Such LEEs exhibit a small MFP between energy deposits in biological materials and thus lead to a very large absorbed dose when considering small volumes (i.e., less than 1 μm in diameter) [44]. For instance, given that ^{125}I can be incorporated directly into DNA using ^{125}I-deoxyuridine [6], and assuming $R \sim 0.3$ nm in Eq. (4), such an inclusion would be much more beneficial with a tenfold increase in the dose values of Table II. Thus quite different biological responses are to be expected depending on the type of Auger event and its molecular location. The present model represents a simple step towards the evaluation of the corresponding nanoscopic doses. More generally, trying to correlate such nanoscopic doses to cell death or biological responses with the purpose of establishing RBE should make it possible to generate specific weighting factors for cell constituents, cells, and tissues.

ACKNOWLEDGMENTS

M. Bazin gratefully acknowledges financial support from the Canadian Institutes of Health Research (CIHR) in the form of a postdoctoral research award. This research was also supported by the CIHR.

[1] M. N. Gaze, Phys. Med. Biol. **41**, 1895 (1996).
[2] T. E. Wheldon, Phys. Med. Biol. **45**, 77 (2000); a review see *Monoclonal Antibody and Peptide-Targeted Radiotherapy of Cancer*, edited by R. M. Reilly (Wiley, New York, 2010).
[3] R. M. Sharkey and D. M. Goldenberg, Cancer J. Clin. **56**, 226 (2006).
[4] K. G. Hofer, Acta Oncol. **35**, 789 (1996).
[5] L. E. Feinendegen and R. D. Neuman, Int. J. Radiat. Biol. **80**, 813 (2004).
[6] S. J. Adelstein, A. I. Kassis, L. Bodei, and G. Mariani, Cancer Biother. Radiopharm. **18**, 301 (2003).
[7] P. B. Zanzonico, J. Nucl. Med. **41**, 297 (2000).
[8] C. Bousis, D. Emfietzoglou, P. Hadjidoukas, and H. Nikjoo, Phys. Med. Biol. **55**, 2555 (2010).
[9] C. Champion, P. Zanotti-Fregonara, and E. Hindié, J. Nucl. Med. **49**, 151 (2008).
[10] K. Anzai, H. Kato, M. Hoshino, H. Tanaka, Y. Itikawa, L. Campbell, M. J. Brunger, S. J. Buckman, H. Cho, F. Blanco, G. Garcia, P. Limão-Vieira, and O. Ingólfsson, Eur. Phys. J. D **66**, 36 (2012).
[11] D. B. Jones, S. M. Bellm, F. Blanco, M. Fuss, G. García, P. Limão-Vieira, and M. J. Brunger, J. Chem. Phys. **137**, 074304 (2012).
[12] C. Champion, Phys. Med. Biol. **55**, 11 (2010).
[13] I. Baccarelli, F. A. Gianturco, A. Grandi, and N. Sanna, Int. J. Quantum Chem. **108**, 1878 (2008).
[14] M. Vinodkumar, K. N. Joshipura, C. Limbachiya, and N. Mason, Phys. Rev. A **74**, 022721 (2006).
[15] Y. Itikawa and N. Mason, J. Phys. Chem. Ref. Data **34**, 1 (2005).
[16] H. Nikjoo and L. Lindborg, Phys. Med. Biol. **55**, R65 (2010).
[17] R. L. Loevinger, T. F. Budinger, and E. E. Watson, *MIRD Primer for Absorbed Dose Calculations, Revised* (Society of Nuclear Medicine, New York, 1991).
[18] M. Lepage, S. Letarte, M. Michaud, F. Motte-Tollet, M.-J. Hubin-Franskin, D. Roy, and L. Sanche, J. Chem. Phys. **109**, 5980 (1998).
[19] S.-P. Breton, M. Michaud, C. Jäggle, P. Swiderek, and L. Sanche, J. Chem. Phys. **121**, 11240 (2004).
[20] P. L. Lévesque, M. Michaud, and L. Sanche, Nucl. Instrum. Methods Phys. Res., Sect. B **208**, 225 (2003).
[21] P. L. Lévesque, M. Michaud, W. Cho, and L. Sanche, J. Chem. Phys. **122**, 224704 (2005).
[22] P. L. Lévesque, M. Michaud, and L. Sanche, Rev. Sci. Instrum. **76**, 103901 (2005).
[23] P. L. Lévesque, M. Michaud, and L. Sanche, J. Chem. Phys. **122**, 094701 (2005).
[24] R. Panajotovic, M. Michaud, and L. Sanche, Phys. Chem. Chem. Phys. **9**, 138 (2007).
[25] M. Bazin, M. Michaud, and L. Sanche, J. Chem. Phys. **133**, 155104 (2010).
[26] M. Michaud, M. Bazin, and L. Sanche, Int. J. Radiat. Biol. **87**, 472 (2011).
[27] M. Michaud, M. Bazin, and L. Sanche, J. Chem. Phys. **137**, 115103 (2012).
[28] G. Sgouros, J. Nucl. Med. **46**, 18 (2005).
[29] M. Bardiès and M. J. Myers, Phys. Med. Biol. **41**, 1941 (1996).
[30] M. Bardiès, G. Flux, M. Lassmann, M. Monsieurs, S. Savolainen, and S. E. Strand, Nucl. Instrum. Methods Phys. Res., Sect. A **569**, 467 (2006).
[31] R. W. Howell, J. Nucl. Med. **35**, 531 (1994).
[32] R. W. Howell, B. W. Wessels, R. Loevinger, E. E. Watson, W. E. Bolch, A. B. Brill, N. D. Charkes, D. R. Fisher, M. T. Hays, J. S. Robertson, J. A. Siegel, and S. R. Thomas, J. Nucl. Med. **40**, 3S (1999).
[33] E. Pomplun, J. Booz, and D. E. Charlton, Radiat. Res. **111**, 533 (1987).
[34] M. Terrisol, S. Edel, and E. Pomplun, Int. J. Radiat. Biol. **80**, 905 (2004).
[35] M. Inokuti, Int. J. Quantum Chem. **57**, 173 (1996).
[36] For a review see, L. Sanche, in *Radiation Damage in Biomolecular Systems*, edited by G. García Gómez-Tejedor (Springer, New York, 2012).
[37] H. S. W. Massey, *Negative Ions* (Cambridge University Press, London, 1976).
[38] ICRP 53, *Radiation Dose to Patients From Radiopharmaceuticals*, ICRP Publication 38 (Pergamon, Oxford, 1992).
[39] E. Hindie, N. Colas-Linhart, A. Petiet, and B. Bok, J. Nucl. Med. **29**, 1118 (1988).
[40] M. R. B. Puncher and P. J. Blower, Eur. J. Nucl. Med. **21**, 1347 (1994).
[41] G. M. Makrigiorgos, S. J. Adelstein, and A. I. Kassis, J. Nucl. Med. **30**, 1856 (1989).
[42] R. W. Howell, Med. Phys. **19**, 1371 (1992).
[43] J. L. Humm, R. W. Howell, and D. V. Rao, Med. Phys. **21**, 1901 (1994).
[44] M. Faraggi, I. Gardin, C. de Labriolle-Vayley, J. L. Moretti, and B. Bok, J. Nucl. Med. **35**, 113 (1994).